Astron. Astrophys. 230, L29–L32 (1990)

ASTRONOMY AND ASTROPHYSICS

Letter to the Editor

First diffraction-limited astronomical images with adaptive optics

G. Rousset[1], J.C. Fontanella[1], P. Kern[2], P. Gigan[2], F. Rigaut[2], P. Léna[2], C. Boyer[3], P. Jagourel[3], J.P. Gaffard[3] and F. Merkle[4]

[1] Office National d'Etudes et de Recherches Aérospatiales (ONERA), BP 72, F-92322 Châtillon Cedex, France
[2] Observatoire de Paris et Université Paris 7, Unité Associée au CNRS no. 264, F-92195 Meudon Cedex, France
[3] LASERDOT, Route de Nozay, F-91460 Marcoussis, France
[4] European Southern Observatory (ESO), Karl-Schwarzschild-Strasse 2, D-8046 Garching bei München, Federal Republic of Germany

Received December 1, accepted December 8, 1989

SUMMARY. For the first time in ground-based astronomy, diffraction-limited imaging through atmospheric turbulence is achieved in real time with adaptive optics. The "COME-ON" adaptive optics prototype system has been tested at the 1.52 m telescope of the Observatoire de Haute Provence, giving diffraction-limited images at near infrared wavelengths (2.2 to 5 μm). This Letter presents the first results and their analysis, which demonstrate the considerable gain in resolution and sensitivity achieved by adaptive optics. A close binary (γ_2 And) is resolved at 2.23 μm, when an other star (γ_1 And), 9.6 arcsec apart, is used as reference for the wavefront sensing at 0.6 μm.

Key words: image processing - infrared radiation - instruments - observational methods - seeing.

1. INTRODUCTION

Although the potential of adaptive optics for ground-based astronomical imaging, initially proposed by Babcock (1953), is now widely acknowledged to overcome the atmospheric turbulence limitation, its practical feasibility has been questioned for years. First tests were performed several years ago at visible wavelengths (Buffington et al., 1977; Hardy, 1981). A review of the recent development in adaptive optics for astronomy can be found in the proceedings of the conference on "Active Telescope Systems" (Roddier, 1989). An adaptive optics system, the so-called "COME-ON" prototype system, has been built to demonstrate the performance of this technique for astronomy. The first results have been obtained at the 1.52 m telescope of the Observatoire de Haute-Provence (CNRS) in the near infrared (IR): 1.6 to 5 μm. They establish that diffraction-limited imaging with a telescope of significant size, can be achieved above 2.2 μm under average seeing conditions.

2. THE INSTRUMENT

The instrument (Kern et al, 1989) combines the following main components:
a) A Shack-Hartmann wavefront sensor made of 5 × 5 subapertures and working at visible wavelengths: its camera is a Reticon 100 × 100 photodiode array equipped with a RTC intensifier. The S20R photocathode has a peak sensitivity at λ_0 = 0.6 μm and a bandwidth $\Delta\lambda$ = 0.4 μm.
b) A deformable mirror driven by 19 piezo-electric actuators of ± 7.5 μm stroke: the pupil diameter on this mirror is 65 mm and the whole diameter of the deformable surface is 130 mm.
c) A tip-tilt mirror, having 6 arcsec peak to peak excursion with 4 marcsec resolution, compensates for the tilt component in the perturbed wavefront.
d) Two coupled computers drive the servo-loop through digital control. The dynamic perturbations of the wavefront are sampled at a 100 Hz rate.
e) A 32 × 32 InSb array camera used for near IR imaging (Lacombe et al., 1989), with 0.236 arcsec pixel size on the sky: any exposure time above 16 ms can be selected. The camera is detector read-out noise limited for $\lambda \leq 2.3$ μm, and thermal background noise limited above.

The frequency response of the system in open-loop extends to 9 Hz (0 dB point). This is equivalent to the bandwidth in closed-loop, and is limited by the computing time.

The system was installed at the Coudé focus of the 1.52 m telescope. The optical train is made of a large number of mirrors leading to some light losses. Moreover the low sensitivity of the intensified Reticon array sets currently the limiting magnitude of the wavefront sensor to m_v = 5, a value which will be significantly improved in the near future.

The wavefront sensor is usually used to determine the error signal feeding the servo-loop, but alternatively may provide a quantitative measurement of the turbulence parameters. The values of the Fried parameter $r_0(\lambda_0)$ and of the atmospheric coherence time $\tau_0(\lambda_0)$ at the sensing wavelength λ_0 are deduced from the angle-of-arrival fluctuations (Roddier, 1981), or from an expansion of the wavefront distortions in Zernike polynomials (Noll, 1976). The measurements are averaged over a time larger than 10 s. The Fried parameter can also be determined from the width of the recorded long exposure images (Fried, 1966).

3. OBSERVATIONS

The observations were carried out by taking, either r_0 and τ_0 measurements and IR images without correction by the adaptive optics system, or IR images with correction. The images are recorded at the standard photometric wavelengths of 1.68 μm (H), 2.23 μm (K), 3.87 μm (L) and 4.75 μm (M) with the standard bandwidth of 0.2 μm (H), 0.3 μm (K), 0.6 μm (L) and 0.4 μm (M). During the nights from October 12 to 23, 1989, bright single stars and binaries have been observed. During this period, seeing was variable from bad (2.4") to good (< 1"), without any significant ground wind.

For general understanding of the results, it should be mentioned that:
a) The images are perfectly stabilized, i.e. within a single pixel, when the servo-loop is locked. Average images are therefore obtained without any shift-and-add treatment. This is due to a proper feedback control of the tip-tilt mirror taking into account all pointing and tracking errors.
b) The data processing of the images has been limited to background subtraction and dead pixel removal (Lacombe et al., 1989).

c) At the shortest wavelengths (H and K bands), the selected pixel size causes an undersampling of the diffraction figure in the image plane. The resulting effect is an aliasing of the Modulation Transfer Function (MTF).

The first set of images (Fig. 1) shows ξ Cygnus (m_v = 3.7) at four bands without and with closed-loop correction. Averaging of N recorded images is done, N is of the order of a few hundreds and the exposure time t_p of each recorded image is around 100 ms (see Fig. 1 caption). The averaged images are therefore equivalent to long exposure images. For each band, the comparison of the upper images (1) with the central ones (2) reveals the gain in energy concentration obtained with the adaptive optics correction, as the comparison of the lower images (3) with the central ones reveals the gain in width. The uncorrected images are elongated by a static aberration of the telescope in the Coudé path. During this 90 min sequence, the $r_0(\lambda_0)$ value, at λ_0 = 0.6 μm, is between 13 and 8 cm and the $\tau_0(\lambda_0)$ is of the order of 10 ms, as measured by the wavefront sensor.

From the data in Figure 1, the system behavior in the turbulence conditions encountered during this night can be described versus wavelength by: first, the energy concentration efficiency in terms of Strehl ratio (Fig. 2) and second, the gain in resolution (Fig. 3). The Strehl ratio is defined as the peak intensity in the averaged image by the peak intensity in the perfect diffraction-limited image. In Figure 2, Curve 1 presents the *adaptive optics efficiency* defined as the ratio, $\eta_{ao} = S_c/S_u$, of the Strehl ratio S_c with closed-loop correction (Curve 2) and of the Strehl ratio S_u without correction (Curve 3). η_{ao} has a maximum at a wavelength λ_{me} = 2.23 μm (η_{ao} = 6.7). The wavelength λ_{me} is characteristic of the performance of the whole instrument (adaptive optics and telescope) for a given condition of the atmospheric turbulence. Above λ_{me}, the Strehl ratio S_c is higher than 60 %. At shorter wavelengths, the correction becomes partial: S_c < 60 %.

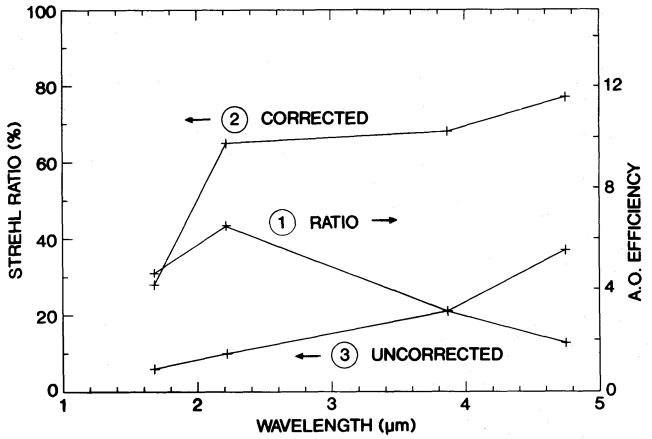

Fig. 2. *Adaptive optics efficiency* and Strehl ratio versus wavelength. Values deduced from Fig. 1. Curve 1 (right-side scale) is the *adaptive optics efficiency*, ratio of the values plotted on Curve 2 (Strehl ratio with correction, left-side scale) over the values plotted on Curve 3 (Strehl ratio without correction, left-side scale).

In Figure 3, the resolution obtained on this unresolved star is presented, defined as the full width at half-maximum (FWHM) of the image. The Curve 1 corresponds to the images without closed-loop correction. It indicates the seeing conditions (about 1") which are known to vary slowly with λ, theoretically as $\lambda^{-1/5}$ (Roddier, 1981). The Curve 2 shows the FWHM obtained with correction. The Curve 3 is λ/D which is the theoretical FWHM of the diffraction pattern of the telescope pupil of diameter D. The resolution with correction reaches the diffraction theoretical behavior for λ_{me} = 2.23 μm. Below this wavelength, the adaptive optics improves the resolution. Above this wavelength, the resolution with correction is always diffraction-limited, hence decreases with the increase of λ: therefore the highest resolution is obtained at λ_{me}. With the above-mentioned seeing value, the r_0 parameter reaches the diameter D for a wavelength λ_{lim} = 7.4 μm. Above λ_{lim}, the telescope is diffraction-limited even without adaptive optics.

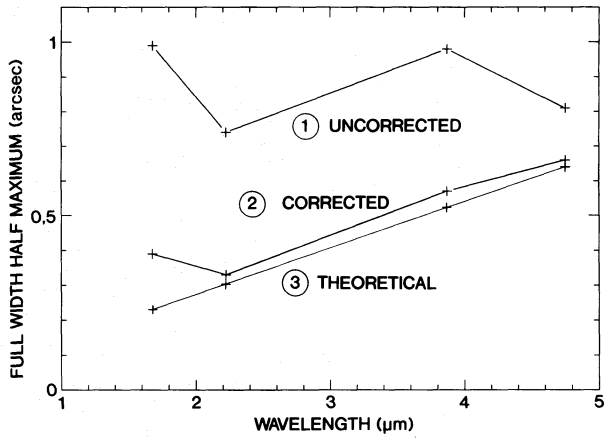

Fig. 3. Resolution, defined as the FWHM of the images of Fig. 1, versus wavelength. Curve 1: without closed-loop correction. Curve 2: with correction. Curve 3: theoretical value λ/D.

Figure 4 gives cross-sections of images obtained at K band. Curve 1 is the theoretical diffraction profile, Curve 2 the result obtained with closed-loop correction and Curve 3 without correction. The corrected image clearly shows the first black and bright rings of the diffraction pattern. During all nights of observation, the first ring of the Airy pattern appears on the corrected images at L and M bands. It also appears partially on most of the images at K band. It should be remarked that the intensity in the bright ring is relatively too high when compared to the theoretical one. This is an effect of the residual phase perturbation induced by the peripheral actuators of the deformable mirror. The spacings between these actuators correspond to spatial frequencies of the order of D/λ in the image. A hexagonal structure is noticeable in the background which is due to the hexagonal arrangement of the actuators of the deformable mirror.

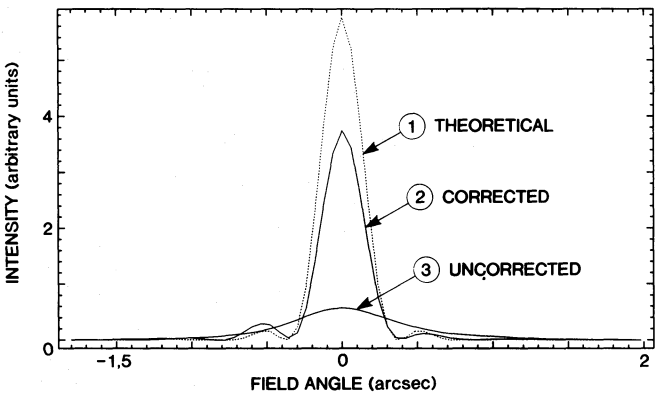

Fig. 4. Cross-sections of the images of Fig. 1 at K band. Curve 1: theoretical diffraction profile. Curve 2: profile with correction. Curve 3: without correction.

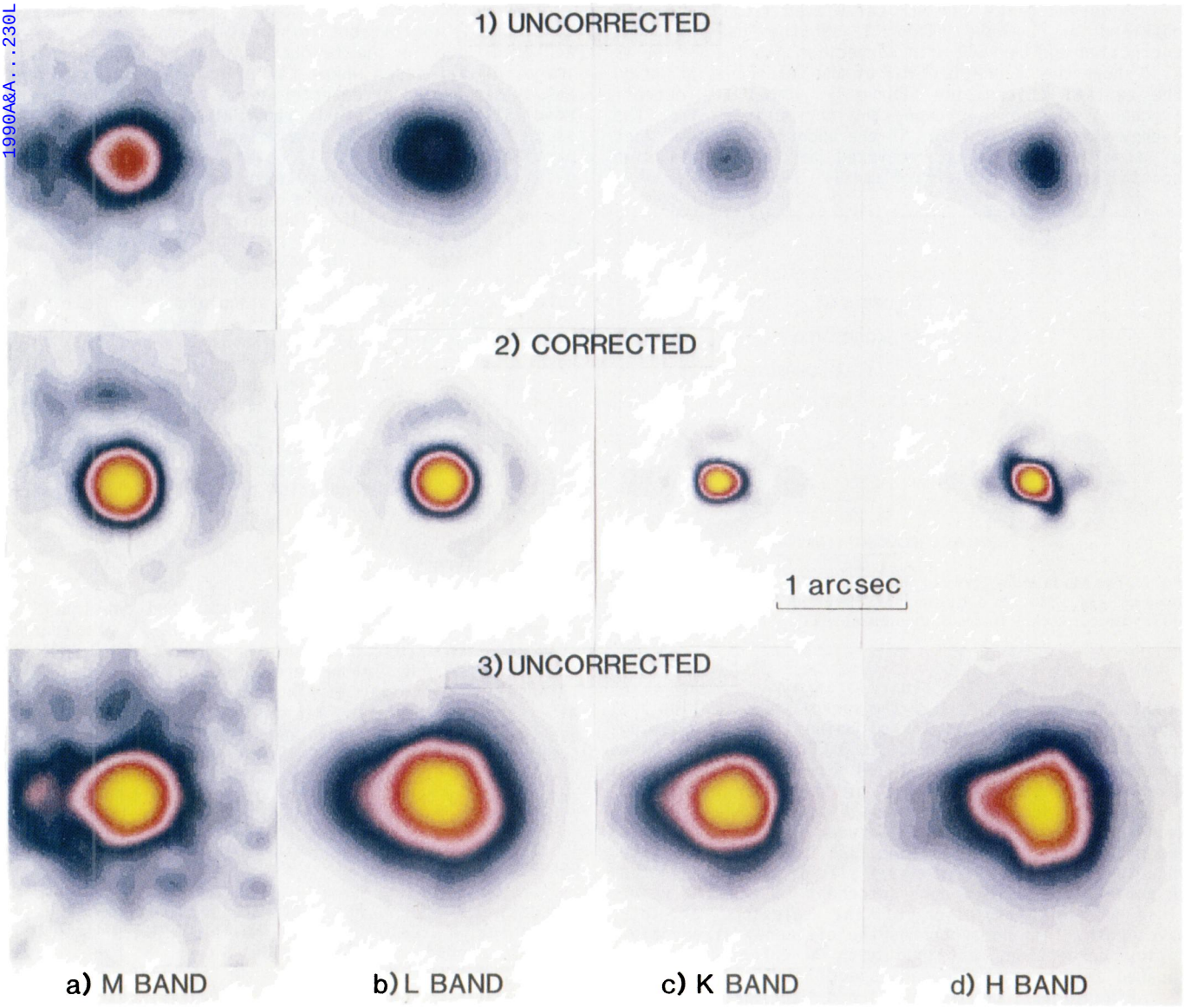

Fig. 1. Images of ξ Cyg (K4 spectral type at air mass = 1.03) in a linear color scale at four spectral bands on October 21, 1989. 1) and 3): the same images without closed-loop correction. 2): the images with correction. For the rows 1) and 2), the same intensity scale is used. For the row 3), the maximum intensity is adjusted to the maximum of the scale. a) M band (λ = 4.75 μm, $\Delta\lambda$ = 0.4 μm) N = 200, t_p = 96 ms, UT = 19h45min. b) L band (λ = 3.87 μm, $\Delta\lambda$ = 0.6 μm) N = 200, t_p = 256 ms, UT = 19h50min. c) K band (λ = 2.23 μm, $\Delta\lambda$ = 0.3 μm), N = 400, t_p = 176 ms, UT = 20h00min. d) H band (λ = 1.68 μm, $\Delta\lambda$ = 0.2 μm), N = 400, t_p = 176 ms, UT = 20h20min.

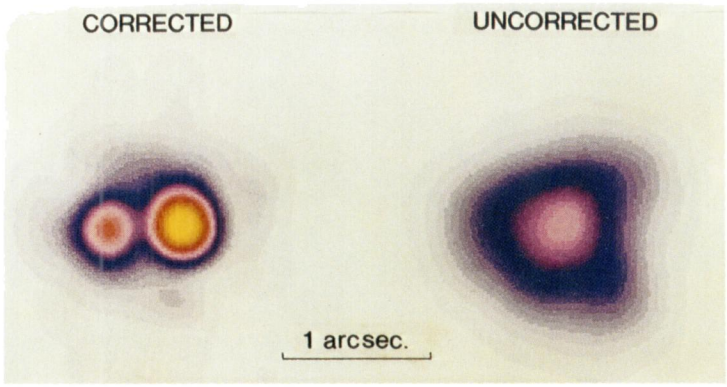

Fig. 6. Images of γ_2 And (A0 spectral type at air mass = 1.08) at K band (magnitudes m_K: 5.3 and 6.1), October 22, 1989, UT = 1h40min, N = 32, t_p = 4 s. Left: corrected image with γ_1 And (9.6" apart) used for the wavefront sensing. Right: uncorrected image in the same linear color scale. $r_0 \simeq$ 12 cm and $\tau_0 \simeq$ 10 ms at λ_0 = 0,6 μm.

Figure 5 gives the MTF calculated from the images obtained at L band. Curve 1 is the case without correction and Curve 2 with correction. In the figure is also shown the theoretical MTF of the telescope including the central obscuration (Curve 3). Until the cut-off frequency of the telescope, the correction raises the energy which is attenuated in the uncorrected case. Most of the information is recovered at medium and high spatial frequencies (Gaffard et al., 1987).

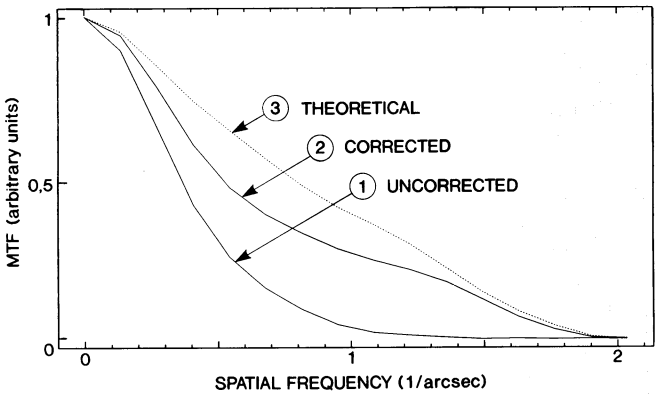

Fig. 5. The Modulation Transfer Function (MTF) calculated from the images of Fig. 1 at L band. Curve 1: MTF without correction. Curve 2: MTF with correction. Curve 3: theoretical MTF.

Figure 6 shows the binary star γ_2 Andromeda at K band (separation 0.55"). For the servo-loop operation the wavefront sensing is performed using the light coming from γ_1 And (m_v = 2.3), which is 9.6" away from γ_2. The separation angle of 9.6" is within the isoplanatic angle which can be estimated to be of the order of 20" at λ = 2.23 μm (Roddier, 1981). In Figure 6, the measured magnitude difference is 0.66 between the two components and the measured separation is 0.50" ± 0.06", the uncertainty is given by the half size of the pixel in the IR camera. The FWHM of each component is 0.32", a value close to the resolution of the telescope at this wavelength. This demonstrates the efficency of adaptive optics correction, obtained with a reference source located away from the imaged object.

Finally it should be mentioned that the servo-loop was easily locked and ran with a high stability, for any reference source brighter than the limiting magnitude of the wavefront sensor, and irrespective of the encountered seeing conditions. This demonstrates the robustness of the adaptive optics system control.

4. CONCLUSION

The purpose of these first observations was to demonstrate the applicability of adaptive optics to astronomy. One has to recall that this version of the instrument was not optimized for high photometric efficiency. Its goal was a first evaluation of the correction performance of adaptive optics in actual turbulence conditions at an astronomical site.

First, the successfully performed observations show that the full gain in resolution, leading to diffraction-limited images, is obtained at a wavelength of maximum efficiency λ_{me} and above. The value of this wavelength depends on the turbulence conditions, the telescope diameter, the number of actuators on the deformable mirror and the band pass of the loop. For the presented results, λ_{me} is equal to 2.23 μm and corresponds to the highest feasible resolution. The coherence of the wave is fully recovered in the central core of the image, a major step for the combinaison of large telescopes.

Second, a gain in sensitivity is obtained. A considerable improvement in signal-to-noise ratio can be achieved, due to the bright maximum of the sharpened image, in all cases where the signal-to-noise ratio is set by background or detector noise as for the presented results. The gain in Strehl ratio at λ_{me} for 0.75" seeing is of the order of 6.7. At wavelengths shorter than λ_{me}, partial correction is still obtained with a significant gain in Strehl ratio. The consequence of this gain in sensitivity is an increase of the limiting magnitude and/or a reduction of the exposure time. These advantages will also be beneficial for spectroscopy.

Third, corrected images of faint objects may be obtained by using, for the wavefront sensing, a bright reference star located in the isoplanatic angle of the object. In such a case, the exposure time can be significantly increased allowing the record of a high resolution images of faint objects.

In spring 1990, the "COME-ON" prototype system will be installed on the ESO 3.6 m telescope at La Silla (Chili). A systematic study of isoplanacity of this site will be undertaken, as well as astronomical observations. The results will allow to specify the adaptive optics system for the next generation of giant telescopes such as the European Very Large Telescope.

ACKNOWLEDGEMENTS

This project was a joint design and construction program. It was carried out under: the ESO contracts 18407/4001 and 22009/4001, and the contract 86.E.0401 of the Ministère de la Recherche et de la Technologie (France). It received also financial supports from the Ministère de l'Education Nationale and Institut National des Sciences de l'Univers and technical help from the Service des Prototypes, CNRS/Bellevue (France). Early developments of adaptive optics components were independently supported by the Direction des Recherches, Etudes et Techniques, Ministère de la Défense (France).

REFERENCES

Babcock, H.W.: 1953, *Publ. Astron. Soc. Pac.* **65**, 229
Buffington, A., Crawford, F.S., Muller, R.A., Orth, C.D.: 1977, *J. Opt. Soc. Am.* **67**, 304
Fried, D.L.: 1966, *J. Opt. Soc. Am.* **56**, 1372
Gaffard, J.P., Boyer, C.: 1987, *Appl. Opt.* **26**, 3772
Hardy, J.W.: 1981, in *High Angular Resolution at Infrared and Optical Wavelength*, ESO Conference, Garching, 25
Kern, P., Léna, P., Gigan, P., Fontanella, J.C., Rousset, G., Merkle, F., Gaffard, J.P.: 1989, *SPIE Proc.* **1114**, 54, and References herein
Lacombe, D., Tiphène, D., Rouan, D., Léna, P., Combes, M.: 1989, *Astron. Astrophys.* **215**, 211
Noll, R.J.: 1976, *J. Opt. Soc. Am.* **66**, 207
Roddier, F., (Ed.): 1989, *SPIE Proc.* **1114**
Roddier, F.: 1981, in *Progress in Optics* (Wolf, E., Ed.), North Holland, 283